

**Membranes in rod solutions:  
a system with spontaneously broken symmetry**

K. Yaman and P. Pincus

*Department of Physics, University of California, Santa Barbara, California 93106–9530*

C. M. Marques

*R.P.-C.N.R.S., Complex Fluid Laboratory UMR166, Cranbury, NJ 08512–7500, USA*

(May 2, 2019)

Abstract

We consider a dilute solution of infinitely rigid rods near a curved, perfectly repulsive surface and study the contribution of the rod depletion layer to the bending elastic constants of membranes. We find that a spontaneous curvature state can be induced by exposure of *both* sides of the membrane to a rod solution. A similar result applies for rigid disks with a diameter equal to the rod's length. We also study the confinement of rods in spherical and cylindrical repulsive shells. This helps elucidate a recent discussion on curvature effects in confined quantum mechanical and polymer systems.

87.22.B, 82.70.Dd

The elastic properties of fluid membranes are among the ruling factors in the physics of many biological and surfactant systems such as cell membranes, vesicles, lyotropic liquid crystals or microemulsions [1]. When macromolecular species are also present in such systems, the interactions between the membranes and the macromolecules change the bare elastic constants. Recent studies have explored contributions from adsorption [2–6], depletion [4–6] or end-grafting [5,7–9] of flexible polymers. In all of these cases, exposure of both sides of the membrane to a solution results in a modification of the bending and splay moduli  $K$  and  $\bar{K}$ , the sign of the contribution depending on the possibility of surface-bulk equilibration. For instance, depleted or adsorbed polymers reduce  $K$  and increase  $\bar{K}$ , whereas the reverse holds for end-grafted polymers.

Interest in solutions of rigid macromolecules can be traced to the extraction of tobacco mosaic virus (TMV) [10] and to the subsequent observation of the nematic phase in TMV solutions [11], later explained by the seminal theory of Onsager [12]. Rod shaped particles in the colloidal range have since been studied in a large variety of mineral and organic systems [13], they are also present in the biological realm where examples range from TMV-like virus to fibrils of amyloid  $\beta$ -protein, the molecular agent at the origin of the Alzheimer disease. The surface interactions of rigid macromolecules were first studied by Asakura and Oosawa [15] who showed that the steric depletion of the molecules at a flat surface increases the interfacial energy of the system, implying that two surfaces brought to separations smaller than a rod length will experience an attractive force. The theory of depletion interactions for rods have since been extended to include ordering effects of the bulk phase [16] or effects of rod-rod excluded volume interactions [17]; but it has been mostly [18] devoted to flat geometries. In this letter we extend the original Asakura and Oosawa theory to include effects of surface curvature and determine the contribution of the rod depletion layer to the elastic constants of the membranes. An important reason for considering this case can be better understood by comparing the order of magnitudes of changes in  $K$  and  $\bar{K}$  caused by depleted layers of rods with those caused by spherical particles. In a solution of colloidal spheres of radius  $r_0$  and particle number density  $\rho_b$ , the typical scale of the energy density is  $k_B T \rho_b$ .

Corrections to the interfacial energy are thus of the order  $\Delta\gamma \simeq k_B T \rho_b r_0$ . On other hand, interfacial tensions in most liquids are of the order of  $\gamma_0 \simeq k_B T / a^2$  where  $a$  is a microscopic size. For instance for  $a \sim 0.1\text{nm}$ ,  $\gamma_0$  is of the order of tens of mN/m. The corrections due to the depletion of spherical particles are thus a factor  $(a/r_0)^2$  lower than typical interfacial tensions even at order unity volume fractions  $\phi = \rho_b (4\pi/3) r_0^3$ . Curvature corrections to the interfacial energy can generally be written as  $\Delta\gamma \simeq k_B T \rho_b r_0 (1 + C_1 r_0/R + C_2 r_0^2/R^2)$ , with  $R$  the radius of curvature and  $C_1, C_2$  two numerical constants. This leads to modifications of the bare elastic constants of the order of  $\Delta K \simeq k_B T \rho_b r_0^3$ : at the upper concentration limit  $\rho_b \sim 1/r_0^3$ , these corrections are only of order  $k_B T$ , a value at the lower end of the range [19],  $1 - 20k_B T$ , of most bare elastic constants. In the case of a rod solution with rod number density  $\rho_b$ , the upper concentration limit of the isotropic solution is the Onsager concentration  $\rho_b^* = 4.2/(L^2 D)$  [12], with  $L$  the length of the rod and  $D$  its diameter. The contributions to the interfacial tension are now of the order  $\Delta\gamma \simeq k_B T \rho_b L$ , but even for rod diameters of order of the microscopic length  $a$  the contribution to the interfacial tension of rod solutions at the Onsager concentration is still a factor  $(a/L)$  smaller than typical interfacial tension values. However, modifications of the elastic constants are here of order  $\Delta K \simeq k_B T \rho_b L^3$ , a factor  $(L/D)$  larger than  $k_B T$ . Therefore, even rather rigid phospholipid membranes with elastic constants as large as  $20k_B T$  may have their rigidities modified substantially at low rod concentrations where rod-rod interactions are negligible. We remark also that the steric surface interactions are identical for rigid rods and rigid disks if one takes the rod's length and the disk's diameter to be the same; however the disk system does not enjoy the above-mentioned  $L/D$  enhancement.

We consider an ideal gas of rods of length  $L$  in the presence of flat and curved surfaces which repel the rods. We parameterize the possible rod configurations by the center of mass coordinates,  $\vec{r}$ , and the two angles specifying in which direction the rod points,  $\omega \equiv (\theta, \phi)$ . For sake of simplicity the thickness of the rods is taken to be zero. The relevant potential describing the thermodynamics of the system can be written as

$$\Omega[\rho(\vec{r}, \omega)] = \int d\vec{r} \int d\omega \rho(\vec{r}, \omega) [\log(v \rho(\vec{r}, \omega)/e) - (\mu_b - U_{ext}(\vec{r}, \omega))] \quad (1)$$

where  $v$  is some normalization volume,  $\mu_b$  is the solution chemical potential, and  $U_{ext}$  is the hard wall interaction potential that is either infinite or zero, depending on whether the configuration of the rod is allowed by the ‘hard wall’ requirement or not. Functional minimization of  $\Omega$  with respect to  $\rho(\vec{r}, \omega)$  gives the equilibrium density profile:

$$\rho(\vec{r}, \omega) = \frac{e^\mu}{v} e^{-U_{ext}(\vec{r}, \omega)} \equiv \frac{\rho_b}{4\pi} e^{-U_{ext}(\vec{r}, \omega)} \quad (2)$$

The local, position dependent, number density of particles  $\rho(\vec{r})$  is simply the sum over all allowed angular configurations of  $\rho(\vec{r}, \omega)$ . The excess surface energy is then calculated from

$$\Delta\gamma = \frac{\Omega[\rho(\vec{r}, \omega)] - \Omega[\rho(z \rightarrow \infty, \omega)]}{S} = \int dz (\rho_b - \rho(z)) J(z, R) \quad (3)$$

where  $S$  is the surface area,  $z$  the perpendicular distance from the surface and  $J(z, R)$  a phase space factor, which depends on the geometry. For flat surfaces  $J(z, R) = 1$ , for cylinders of radius  $R$ ,  $J(z, R) = 1 + z/R$ , and for spheres  $J(z, R) = (1 + z/R)^2$ . From equation (3) it is clear that differences between the excess energy of a flat and a curved surface depend on two factors. The first is the configurational part measured by the differences in the rod density profiles, the second one is associated with the space available to the center of mass in the neighborhood of the surface, and is measured by  $J(z, R)$ . In the case of hard sphere solutions, where there is no coupling between configuration and curvature, only  $J(z, R)$  is responsible for energy differences; ( $\rho(z) = \rho_b \Theta(z - L/2)$ , independent of geometry). It is easy to show that in that case one has  $\Delta\gamma = k_B T \rho_b r_0 (1 + r_0/(2R))$  for cylindrical surfaces and  $\Delta\gamma = k_B T \rho_b r_0 (1 + r_0/R + r_0^2/(3R^2))$  for spherical ones. Following the usual procedure [1] one then finds the corrections to the elastic constants of a membrane exposed to a colloidal solution:  $\Delta K = 0$  and  $\Delta \bar{K} = 2/3 k_B T \rho_b r_0^3$ .

Figure 1 shows the angular geometrical constraints for a rod close to a flat or curved surface. When the center of mass is at a perpendicular distance larger than  $L/2$  from the

surfaces, the direction of the rod is not constrained. For distances  $0 < z < L/2$  only a fraction of the solid angle is available to the rod. For rods outside a curved geometry a second distance  $z_c^o$  must be defined: for  $z_c^o < z < L/2$  the rod touches the surface with its end, whereas for distances smaller than  $z_c^o$  the rod touches the surface somewhere along its length. Inside a curved geometry yet a different length  $z_c^i$  must be defined, below which the rod is geometrically not allowed. Performing the angular integrations one gets the density profiles plotted in figure 2. As expected rods outside a spherical curved surface have a larger density than rods close to a flat surface. Conversely, rods inside a spherical surface have a smaller density than rods close to the flat surface. The density profile of rods close to cylindrically bent surfaces is identical to the spherical profile when the rods are oriented perpendicularly to the cylinder axis, and to the flat profile when the rods are oriented along the cylinder's axis. Intermediate angles interpolate smoothly between the two limits. A notable feature of the density profiles is that they are non-analytic functions of the curvature. For instance, the inner part ( $z < z_c^o$ ) of the external profile depends on the square root of the curvature, and the internal profile has a cutoff at  $z_c^i$ . This implies that even for large radii of curvature one cannot simply obtain the internal profiles from the external one by a  $R \rightarrow -R$  transformation. Integration of the profiles lead to the following contributions to the interfacial energies:

$$\Delta\gamma_{\text{out}} = k_b T \rho_b \frac{L}{4} \quad (4)$$

for rods outside spheres and cylinders, or close to flat surfaces;

$$\Delta\gamma_{\text{in}} = k_b T \rho_b \frac{L}{4} \left( 1 - \alpha \frac{L^2}{R^2} \right) \quad (5)$$

for rods inside spheres ( $\alpha = 1/12$ ) and cylinders ( $\alpha = 1/32$ ). Results for the outside configuration are exact. For the inside configuration results are exact for spheres, and perturbative to second order in  $1/R$ , for cylinders. Equations (4) and (5) bear a few interesting consequences. For instance equation (4) implies that the excess free energy of a convex volume immersed in a rod solution does not depend on how the surface of the object is curved, but

only on its area. Also, equation (5) indicates that flexible membranes which expose one surface to a rod solution will spontaneously bend towards the solution. Note however that there is no spontaneous curvature in the usual sense of a contribution to the energy linear in  $1/R$ . When the membrane is immersed in the solution (exposure of both sides of the membrane) the total surface energy excess is given by the sum of the two contributions  $\Delta\gamma_{\text{in}}$  and  $\Delta\gamma_{\text{out}}$ . Curving the surface still decreases the total free energy, but in this symmetric situation there is no preferred side toward which the membrane should bend. Immersion will therefore spontaneously break the symmetry of the system. To the extent that the non-analytic character of the total free-energy can be neglected (there is a finite discontinuity in the second derivative at  $1/R = 0$ ), the following contributions to the membrane elastic constants can be extracted

$$\Delta K = -k_B T \rho_b \frac{L^3}{64} = -k_B T \frac{\rho_b}{\rho_b^*} \frac{1}{15.2} \frac{L}{D}, \quad (6)$$

$$\Delta \bar{K} = k_B T \rho_b \frac{L^3}{96} = k_B T \frac{\rho_b}{\rho_b^*} \frac{1}{22.9} \frac{L}{D}. \quad (7)$$

One finds thus a reduction in  $K$  and an increase in  $\bar{K}$  - this favors the formation of saddle structures (for instance, cubic phases with periodic minimal surfaces). This is similar to other depletion and equilibrium adsorption problems, but as explained above the amplitude of the contributions in this system is very large (of order of  $L/D$  times larger than  $k_b T$ , a value to be compared for instance to  $k_b T \ln N$  for adsorbed polymers with polymerization index  $N$ ).

In a confined geometry, e.g. in ordered stacks of membranes (lyotropic smectics), in multilamellar vesicles or between any other two surfaces separated by some distance  $d$  the rod configurations are restricted by two constraints. If the distance  $d$  is larger than the rod length the confinement effect can be calculated from the above results simply by summing the effects of two non-overlapping depletion layers. If the surfaces are at a distance smaller than the rod's length the two depletion layers overlap, and one needs to compute two-surface effects specifically. The overlap of the rod depletion layers is known to lead to

an attractive force between the two surfaces, but recent calculations that include rod-rod excluded volume interactions in flat geometries show that a repulsive force can set in at distances of the order of the rod length [17]. Our method can in principle be applied to the evaluation of the force between two convex spherical or cylindrical surfaces, but we postpone presentation of those results to a forthcoming paper and concentrate here on the simpler case of confinement in spherical or cylindrical hard shells. This problem is related to a recent discussion of the curvature effects in confined quantum mechanical or macromolecular systems. Indeed, if a quantum mechanical particle is confined in a one or two dimensional manifold embedded in three dimensions, its movement along that manifold will be described by the usual Schrödinger equation with an additional curvature dependent potential. For instance a quantum particle moving in a confinement tube will always be attracted by curved regions of that tube. A quantum particle in a two dimensional manifold will experience an extra potential [20],  $U = -\frac{\hbar^2}{2m} \frac{1}{4} \left( \frac{1}{R_1} - \frac{1}{R_2} \right)^2$ , with  $R_1$  and  $R_2$  the two principal radii of curvature. Particles will be attracted to curved regions of the surface except when it is spherically bent ( $R_1 = R_2$ ). It has also been shown that such curvature effects propagate into the classical world of statistical mechanics and that the quantum mechanical results hold also for flexible polymers confined into spherically or cylindrically bent gaps [21]. For such a system the difference in the free energy of confined states in curved shells as compared to flat ones is given by  $U = -k_B T \rho_b R_G^2 \frac{1}{4} \left( \frac{1}{R_1} - \frac{1}{R_2} \right)^2$ , where  $R_G^2 \equiv N a^2$ ,  $a$  being the monomer size. Apart from the typical energy scale, these potentials are identical. This identity is due to similarities in the equations governing the behavior of both systems, and in fact holds more generally for other systems containing Laplacians in their equations of motion. In this context it is also interesting to investigate the confinement effect for other classical systems, whose configurations are not determined by Laplacian equations. For confined colloidal particles it is convenient to study these effects by considering open curved gaps, i.e. shells that allow the concentration of their solutions to equilibrate with an external reservoir. Attractive curvature effects under these conditions will show up as an increase of the average concentration in the curved gap as compared to non curved gaps

of identical thickness. For illustration we compute first to second order in  $1/R$  the average concentration for a confined solution of dilute hard spheres:

$$\begin{aligned}\bar{\rho}_{\text{flat}} &= \rho_b \left(1 - 2\frac{r_0}{d}\right) \\ \bar{\rho}_{\text{sph}} &= \rho_b \left(1 - 2\frac{r_0}{d}\right) \left(1 - \frac{(d-r_0)}{3} \frac{r_0}{R^2}\right) \\ \bar{\rho}_{\text{cyl}} &= \rho_b \left(1 - 2\frac{r_0}{d}\right)\end{aligned}\tag{8}$$

A spherical curvature is therefore repulsive to the particles, whereas the cylindrical bent shells behave as flat gaps. For the confined rod-solution we report the value of the average concentration for the flat, spherical and cylindrical geometries when the surface separation is equal to the rod length ( $d = L$ )

$$\begin{aligned}\bar{\rho}_{\text{flat}}(d = L) &= \frac{\rho_b}{2} \\ \bar{\rho}_{\text{sph}}(d = L) &= \frac{\rho_b}{2} \left(1 - \frac{1}{16} \frac{1}{R^2}\right) \\ \bar{\rho}_{\text{cyl}}(d = L) &= \frac{\rho_b}{2} \left(1 + \frac{1}{128} \frac{1}{R^2}\right)\end{aligned}\tag{9}$$

At this separation the spherical shell is repulsive for the rod particles, and the cylindrical shell is attractive. For lower distances both shells become repulsive. Results for several different systems are presented in Table I. Despite quantitative differences, it is apparent that cylindrical shells are always more attractive than spherical shells. Comparison between the hard spheres case and the rod and the polymer case also indicate that the coupling between curvature and configuration reinforces the primary effect of volume exclusion. Note however that all the systems quoted in the Table have a repulsive interaction with the confining walls. Further insight into this problem and a test for the generality of the conclusions drawn here will require the study of systems where the particles are attracted to or bound to the confining walls. Work under progress includes for instance end-grafted polymers and adsorbed rod-like particles.

This work was partially supported by CNRS and NATO fellowships, and NSF grants DMR-9624091 and MRL-DMR-9632716. Acknowledgment is also made to the donors of the Petroleum Research Fund, administered by the ACS, for support of this research (#29306-AC7).

## REFERENCES

- [1] S. A. Safran, *Statistical Thermodynamics of Surfaces, Interfaces and Membranes* (Addison-Wesley, 1994).
- [2] Gennes, P.G. *J. Phys. Chem.* **94**, 8407 (1990).
- [3] Brooks, J.T.; Marques C.M.; Cates M.E. *Europhys. Lett.* **14**, 713 (1991).
- [4] Brooks, J.T.; Marques C.M.; Cates M.E. *J. Phys. II (Paris)* **6**, 673 (1991).
- [5] R. Podgornik *Europhys. Lett.* **21**, 245 (1993).
- [6] Eisenriegler, E.; Hanke, A.; Dietrich, S. preprint.
- [7] Cantor, R. *Macromolecules* **14**, 1186 (1981).
- [8] Milner, S. T.; Witten, T. A.; Cates, M. E. *Macromolecules* **22**, 853 (1989).
- [9] R. Lipowsky *Europhys. Lett.* **30**, 197 (1995).
- [10] Stanley, W.M. *Science* **81**, 644 (1935).
- [11] Bawden F.C.; Pirie, N.W.; Bernal, J.D.; Fankuchen, I. *Nature* **138**, 1051 (1936).
- [12] Onsager, L. *Ann. N.Y. Acad. Sci.* **51**, 627 (1949).
- [13] see Buining, P.A. *J. Phys. Chem.* **97**, 11510 (1993). and references therein.
- [14] Lomakin, A; Chung, D.S.; Benedek, G.B.; Kirschner D.A.; Teplow, D.B. *Proc. Natl. Acad. Sci. USA* **93**, 1125 (1996).
- [15] Asakura, S.; Oosawa, F. *J. Chem. Phys.* **22**, 1255 (1954).
- [16] Poniewierski, A.; Holyst, R. *Phys. Rev. A* **38**, 3721 (1988).
- [17] Mao, Y., A.; Cates, M.E.; Lekkerkerker, H.N.W. *Phys. Rev. Lett.* **24**, 4548 (1995).
- [18] A first attempt at extending the flat results to curved cases can be found in Auvray, L. *J. Phys. (Paris)* **42**, 79 (1981).

- [19] Nelson D.; Piran, T.; Weinberg, S.; Ed. *Statistical Mechanics of Membranes and Surfaces* World Scientific, London (1989).
- [20] Jensen, H.; Koppe, H. *Ann. of Phys.* **63**, 586 (1971).
- [21] Yaman, K.; Pincus, P.; Solis, F.; Witten, T. A. *Macromolecules*, in press.

## FIGURES

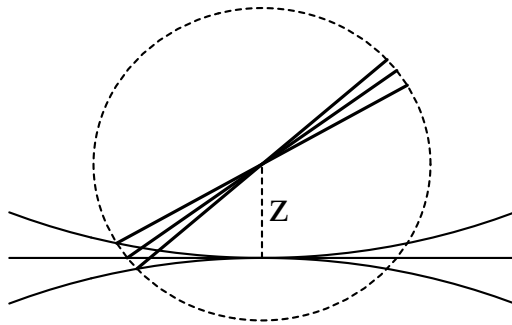


FIG. 1. Configurational space of a rod near a flat surface, outside a curved surface, and inside of a curved surface. The rods are represented at the angle where they touch the surface. The complete allowed angular space is obtained by rotation of the figure around the  $z$ -axis.

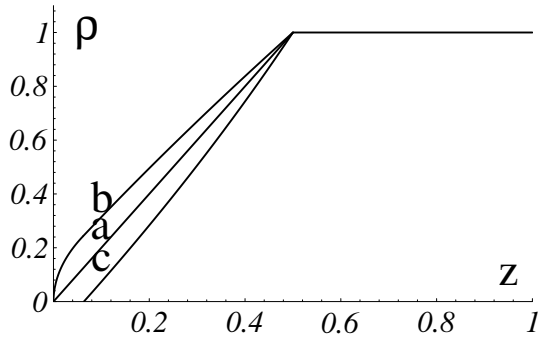


FIG. 2. Profiles for the the rod number density  $\rho(z)$ , in  $\rho_b$  units, close to: **a**) a flat surface; **b**) outside a spherical surface; **c**) inside a spherical surface. In the particular case shown here we have  $L = 1$ ,  $R = 2$ ,  $z_c^o = 0.061$  and  $z_c^i = 0.064$ .

System	Spherical	Cylindrical
Quantum Particle	Neutral	Attraction
Gaussian Chain	Neutral	Attraction
Hard Spheres	Repulsion	Neutral
Rods	Repulsion	Attraction

FIG. 3. Table of the potentials induced by curvature in several systems